

B PHYSICS: PHENOMENOLOGY AND SAMPLE CALCULATIONS*

MIKOŁAJ MISIAK

Institute of Theoretical Physics, Faculty of Physics, University of Warsaw
Pasteura 5, 02-093 Warszawa, Poland

(Received May 4, 2017)

Decays of the B mesons provide us with information on fundamental couplings of the Standard Model, especially those responsible for CP violation. Rare loop-mediated decays are known as sensitive probes of new physics. At present, no deviations from the Standard Model predictions are observed in the radiative ($\bar{B} \rightarrow X_q \gamma$) and leptonic ($B_q^{(0)} \rightarrow \ell^+ \ell^-$) decays, which imposes constraints on some of the relevant Wilson coefficients. On the other hand, sizeable deviations show up in the rare semileptonic decays ($B \rightarrow K^{(*)} \ell^+ \ell^-$) and in the semitauonic decays ($B \rightarrow D^{(*)} \tau \nu$). Their statistical significance is strongly dependent on our estimation of the theoretical uncertainties.

DOI:10.5506/APhysPolB.48.1083

1. Introduction

The major part of B physics amounts to studying mesons containing valence b - or \bar{b} -quarks, together with lighter quarks or antiquarks. Eight of such mesons are stable with respect to the strong and electromagnetic interactions:

$$\begin{array}{llll}
 B^+ (u\bar{b}) & B^0 (d\bar{b}) & \bar{B}^0 (b\bar{d}) & B^- (b\bar{u}) & (m_{B^\pm} \simeq m_{B^0} \simeq 5.28 \text{ GeV}), \\
 & B_s^0 (s\bar{b}) & \bar{B}_s^0 (b\bar{s}) & & (m_{B_s} \simeq 5.37 \text{ GeV}), \\
 B_c^+ (c\bar{b}) & & & B_c^- (b\bar{c}) & (m_{B_c} \simeq 6.29 \text{ GeV}).
 \end{array}$$

Precision studies of the four lightest ones have been performed at the so-called B factories (CLEO, BaBar, Belle) using e^+e^- scattering at the $\Upsilon(4S)$ resonance. In addition, a sizeable amount of data was collected by Belle at

* Presented at the Cracow Epiphany Conference “Particle Theory Meets the First Data from LHC Run 2”, Kraków, Poland, January 9–12, 2017.

$\Upsilon(5S)$ to study the B_s mesons. Such an approach is going to be followed at Belle II that is scheduled to begin collecting data in 2018 [1]. At the high-energy machines (LEP, Tevatron, LHC), one produces all the b -flavoured mesons, as well as baryons, which include $\Lambda_b^0(udb)$, $\Xi_b^0(usb)$, $\Xi_b^-(dsb)$ or $\Omega_b^-(ssb)$.

One of the main motivations for studying the B -meson decays is the determination of those parameters of the Standard Model (SM) that are responsible for CP violation. In the following, I will recall the basic structure of the SM, and the description of CP-violating phenomena in terms of the Cabibbo–Kobayashi–Maskawa (CKM) matrix. Results of the most recent fits for the CKM parameters are going to be summarized, with emphasis on the information from B physics. The status of semileptonic CP asymmetries is going to be reviewed.

Next, I am going to discuss several issues that are unrelated to CP violation: branching ratios of the rare $B_q^{(0)} \rightarrow \ell^+\ell^-$ decays, deviations from the SM predictions in $B \rightarrow K^{(*)}\ell^+\ell^-$ and $B \rightarrow D^{(*)}\tau\nu$ observables, and the current status of $\bar{B} \rightarrow X_q\gamma$.

2. The CKM matrix and CP violation in the SM

The structure of the SM is determined by its gauge group $SU(3) \times SU(2) \times U(1)$ and the field content. The complex scalar fields ϕ reside in the $(\mathbf{1}, \mathbf{2})$ representation of $SU(3) \times SU(2)$. Each of the three generations of left-handed fermion fields ψ is in $(\mathbf{3}, \mathbf{2}) \oplus (\bar{\mathbf{3}}, \mathbf{1}) \oplus (\bar{\mathbf{3}}, \mathbf{1}) \oplus (\mathbf{1}, \mathbf{2}) \oplus (\mathbf{1}, \mathbf{1})$, with the $U(1)$ charges fixed (up to global normalization) by the chiral anomaly cancellation conditions¹. The $U(1)$ charge of the scalar field is then adjusted to allow existence of any gauge-invariant $\phi\psi\psi$ interactions.

Once the fields and symmetries are specified, we write the SM Lagrangian density as a generic dimension ≤ 4 gauge-invariant polynomial in the fields and their derivatives

$$\mathcal{L}_{\text{SM}} = \mathcal{L}_{\text{kin-gauge}} + \mathcal{L}_{\text{Yukawa}} - V(\phi), \quad (2.1)$$

where the three terms on the r.h.s. stand, respectively, for the kinetic and gauge-interaction terms, the Yukawa $\phi\psi\psi$ interaction terms, and the potential for the Higgs field ϕ .

Nowadays, the SM is usually considered as a part of a low-energy effective theory called the Standard Model Effective Field Theory (SMEFT). Its Lagrangian density is obtained by supplementing \mathcal{L}_{SM} with an infinite series of higher-dimensional interactions suppressed by powers of a large scale Λ

$$\mathcal{L}_{\text{SMEFT}} = \mathcal{L}_{\text{SM}} + \frac{1}{\Lambda} \mathcal{L}^{(5)} + \frac{1}{\Lambda^2} \mathcal{L}^{(6)} + \dots \quad (2.2)$$

¹ Including tracelessness of the $U(1)$ generator to avoid the gravitational anomaly.

All the higher-dimensional interactions in SMEFT are believed to be calculable from a more fundamental theory via decoupling of its heavy degrees of freedom, *e.g.*, right-handed neutrinos, heavy gauge bosons or leptoquarks.

It turns out that $\mathcal{L}^{(5)}$ contains only a single interaction term, precisely the one that suffices to explain the measured neutrino mass differences and mixing angles. There are many more interactions in $\mathcal{L}^{(6)}$ [2], and some of them may be responsible for the apparent 2–4 σ deviations from SM predictions in certain low-energy measurements, *e.g.* the muon anomalous magnetic moment or several *B*-physics observables to be discussed in the next sections.

The Higgs potential can be written as $V(\phi) = V_0 + \lambda(\phi^\dagger\phi - v^2/2)^2$. Taking v^2 positive, one finds that the Higgs field acquires a vacuum expectation value that can be chosen as $\langle\phi\rangle = (0, v/\sqrt{2})$, leaving $SU(3) \times U(1)_{\text{em}}$ as the unbroken gauge subgroup. Substituting $\langle\phi\rangle$ into $\mathcal{L}_{\text{Yukawa}}$, one obtains the fermion mass terms

$$\mathcal{L}_{\text{mass}} = -\frac{v}{\sqrt{2}} \left(\bar{u}_R^i Y_u^{ij} u_L^j + \bar{d}_R^i Y_d^{ij} d_L^j + \bar{e}_R^i Y_e^{ij} e_L^j + \text{h.c.} \right), \quad (2.3)$$

where (u_L^j, d_L^j) and (ν_L^j, e_L^j) denote the $SU(2)$ -doublet components of the $(\mathbf{3}, \mathbf{2})$ and $(\mathbf{1}, \mathbf{2})$ fields, while u_R^i, d_R^i and e_R^i stand for charge conjugates of the remaining fermion fields, with the generation indices $i, j = 1, 2, 3$. The complex 3×3 Yukawa coupling matrices Y_u, Y_d, Y_e are the only sources of CP violation in \mathcal{L}_{SM} (2.1).

The fermion mass terms are diagonalized via unitary rotations of the fields in the generation space, *e.g.*, $u_L^{\text{new}} = S_{uL} u_L^{\text{old}}$, giving

$$\mathcal{L}_{\text{mass}} = -\left(\bar{u}_R^i M_u^{ij} u_L^j + \bar{d}_R^i M_d^{ij} d_L^j + \bar{e}_R^i M_e^{ij} e_L^j + \text{h.c.} \right) \quad (2.4)$$

with the 3×3 diagonal fermion mass matrices given by

$$M_u = \frac{v}{\sqrt{2}} S_{uR} Y_u S_{uL}^\dagger, \quad M_d = \frac{v}{\sqrt{2}} S_{dR} Y_d S_{dL}^\dagger, \quad M_e = \frac{v}{\sqrt{2}} S_{eR} Y_e S_{eL}^\dagger. \quad (2.5)$$

At the same time, the *W* boson couplings to quarks become flavour off-diagonal

$$W_\alpha^+ \bar{u}_L^i \gamma^\alpha d_L^j \longrightarrow W_\alpha^+ \bar{u}_L^i \gamma^\alpha V_{ij} d_L^j, \quad (2.6)$$

where $V = S_{uL} S_{dL}^\dagger$ is the unitary CKM matrix. The dimension-four part of the SM action would be CP-invariant if (and only if) the CKM matrix contained no physical phases.

2.1. Parameterizations of the CKM matrix

After removing the unphysical phases by absorbing them into the fields, we can parameterize the CKM matrix V in terms of three angles θ_{ij} and a single phase δ

$$V = \begin{pmatrix} c_{12}c_{13} & s_{12}c_{13} & s_{13}e^{-i\delta} \\ -s_{12}c_{23} - c_{12}s_{23}s_{13}e^{i\delta} & c_{12}c_{23} - s_{12}s_{23}s_{13}e^{i\delta} & s_{23}c_{13} \\ s_{12}s_{23} - c_{12}c_{23}s_{13}e^{i\delta} & -c_{12}s_{23} - s_{12}c_{23}s_{13}e^{i\delta} & c_{23}c_{13} \end{pmatrix},$$

where $c_{ij} = \cos \theta_{ij}$, $s_{ij} = \sin \theta_{ij}$. Next, one passes to the standard Wolfenstein parameterization by defining λ , A , ρ and η via

$$\lambda = s_{12} \simeq 0.22, \quad A = \frac{s_{23}}{s_{12}^2}, \quad \rho = \frac{s_{13}}{s_{23}s_{12}} \cos \delta, \quad \eta = \frac{s_{13}}{s_{23}s_{12}} \sin \delta, \tag{2.7}$$

which implies that

$$c_{12} = \sqrt{1 - \lambda^2}, \quad c_{23} = \sqrt{1 - A^2\lambda^4}, \quad c_{13} = \sqrt{1 - A^2\lambda^6(\rho^2 + \eta^2)}. \tag{2.8}$$

In terms of the Wolfenstein parameters, the CKM matrix becomes

$$\begin{pmatrix} c_{12}c_{13} & \lambda c_{13} & A\lambda^3(\rho - i\eta) \\ -\lambda c_{23} - A^2\lambda^5(\rho + i\eta)c_{12} & c_{12}c_{23} - A^2\lambda^6(\rho + i\eta) & A\lambda^2c_{13} \\ A\lambda^3[1 - c_{12}c_{23}(\rho + i\eta)] & -A\lambda^2c_{12} - A\lambda^4(\rho + i\eta)c_{23} & c_{23}c_{13} \end{pmatrix}. \tag{2.9}$$

Instead of ρ and η , one often works with $\bar{\rho}$ and $\bar{\eta}$ defined by the relation

$$\rho + i\eta = \frac{(\bar{\rho} + i\bar{\eta})\sqrt{1 - A^2\lambda^4}}{\sqrt{1 - \lambda^2}[1 - A^2\lambda^4(\bar{\rho} + i\bar{\eta})]} = (\bar{\rho} + i\bar{\eta}) [1 + \lambda^2/2 + \mathcal{O}(\lambda^4)]. \tag{2.10}$$

The unitarity constraint $V^\dagger V = 1$ gives us 6 independent relations among the CKM matrix elements, *e.g.*,

$$V_{ub}^*V_{ud} + V_{cb}^*V_{cd} + V_{tb}^*V_{td} = 0. \tag{2.11}$$

Such relations define the so-called unitarity triangles, as three complex numbers that sum up to zero form a triangle in the complex plane.

Given that $V_{ub}^*V_{ud} = A\lambda^3(\bar{\rho} + i\bar{\eta}) + \mathcal{O}(\lambda^7)$, $V_{cb}^*V_{cd} = -A\lambda^3 + \mathcal{O}(\lambda^7)$, and $V_{tb}^*V_{td} = A\lambda^3(1 - \bar{\rho} - i\bar{\eta}) + \mathcal{O}(\lambda^7)$, relation (2.11) is practically equivalent to

$$(\bar{\rho} + i\bar{\eta}) - 1 + (1 - \bar{\rho} - i\bar{\eta}) = 0. \tag{2.12}$$

It is the above unitarity triangle that is displayed in the standard fits, to be discussed below.

2.2. Fits for the CKM parameters

Regular updates of the CKM parameter fits are provided by the CKMfitter [3] and UTfit [4] collaborations. Their most recent results are summarized in Table I. The value of $\lambda \simeq |V_{us}|$ is extracted from K and

TABLE I

Fit results for the Wolfenstein parameters by the CKMfitter [3] and UTfit [4] collaborations.

	λ	A	$\bar{\rho}$	$\bar{\eta}$
[3]	$0.22509^{+0.00029}_{-0.00028}$	$0.8250^{+0.0071}_{-0.0111}$	$0.1598^{+0.0076}_{-0.0072}$	$0.3499^{+0.0063}_{-0.0061}$
[4]	0.22497 ± 0.00069	0.833 ± 0.012	0.153 ± 0.013	0.343 ± 0.011

τ decays. Next, the value of $A \simeq |V_{cb}|/\lambda^2$ is determined using both the exclusive and inclusive semileptonic $b \rightarrow c\ell\bar{\nu}$ decay data. Constraints in the $\bar{\rho}-\bar{\eta}$ plane (95% C.L.) are illustrated in Fig. 1. The rings centered at (0,0) come from the semileptonic $b \rightarrow u\ell\bar{\nu}$ decays and from $B^\pm \rightarrow \tau^\pm\nu$. CP violation in $K^0\bar{K}^0$ mixing (ϵ_K) gives rise to the hyperbolic shape in the upper plane. Currently, the most stringent constraints come from the mixing-induced CP violation in $B^0 \rightarrow J/\psi K_S$ ($\sin 2\beta$), as well as from the $B^0-\bar{B}^0$ and $B_s-\bar{B}_s$ mass difference ratio $\Delta m_d/\Delta m_s$ (the ring centered at (1,0)). Additional information on angles α, β, γ of the unitarity triangle (2.12) comes from CP violation in exclusive B^0 decays.

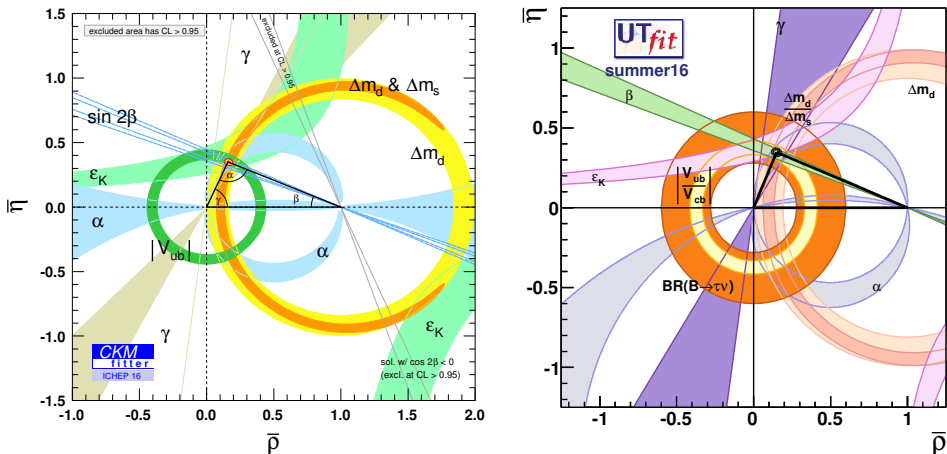


Fig. 1. Experimental constraints in the $\bar{\rho}-\bar{\eta}$ plane, combined by the CKMfitter (left) [3] and UTfit (right) [4] collaborations. They include all the data available in the summer of 2016.

It is evident from the plots in Fig. 1 that the CKM description of flavour- and CP-violating phenomena leads to consistent results. The best-fit point is within the 95% C.L. bound allowed by each of the considered observables. Such a conclusion does not fully coincide with Eq. (35) of Ref. [5] where a 2.3σ tension in ε_K has been found. However, one should take into account that inputs from lattice QCD simulations are crucial for the CKM fits, and estimates of systematic uncertainties in such simulations are always quite delicate.

When discussing the CKM observables, one usually makes a distinction between those that receive contributions from tree-level diagrams in the SM (V_{ub} , γ), and those that are generated only due to loop effects (ε_K , Δm_d , Δm_s or the mixing-induced CP asymmetries). The latter are considered more sensitive to possible contributions from Beyond-SM (BSM) physics. On the other hand, the very loop observables give us currently the most stringent bounds on the location of the unitarity triangle apex $(\bar{\rho}, \bar{\eta})$. Thus, improving the accuracy of the tree-level observable determinations constitutes one of the most important goals in the CKM phenomenology. As far as the angle γ is concerned, its current determination from α is effectively a tree-level enterprise, up to possible violations of isospin symmetry by higher-order electroweak effects. On the other hand, available precision in the determination of $|V_{ub}|$ from $b \rightarrow ul\bar{\nu}$ is limited either by lattice QCD uncertainties (in exclusive decays) or by experimental inaccessibility of the full lepton energy spectrum due to the $b \rightarrow cl\bar{\nu}$ background (in the inclusive case).

2.3. Basics of $B^0\bar{B}^0$ mixing

While CP violation in the $B^0\text{--}\bar{B}^0$ system serves us as an input for the CKM fits, the corresponding phenomena in the $B_s\text{--}\bar{B}_s$ system do not, and they are predicted to be very small within the SM. On the other hand, the dimuon charge asymmetry observed at D0 [6] that deviates from the SM by 3.6σ could be most easily explained by BSM effects in the $B_s\text{--}\bar{B}_s$ mixing. To discuss this issue in more detail, let us recall the basics of neutral meson mixing.

We begin with considering B^0 at rest at the initial time t_0 . For $t > t_0$, the corresponding quantum state is a linear combination of eigenstates of the strong interaction Hamiltonian H_s

$$|\Psi(t)\rangle = a(t) |B^0\rangle + \bar{a}(t) |\bar{B}^0\rangle + \sum_n b_n(t) |n\rangle. \quad (2.13)$$

The $|\bar{B}^0\rangle$ term arises due to the electroweak interactions, with the leading contribution illustrated by the diagram in Fig. 2. Solving the Schrödinger

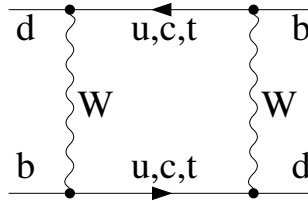


Fig. 2. The box diagram responsible for the $B^0-\bar{B}^0$ mixing.

equation

$$i \frac{d}{dt} |\Psi(t)\rangle = (H_s + H_{\text{weak}}) |\Psi(t)\rangle \tag{2.14}$$

perturbatively in H_{weak} , one arrives at the following differential equation for the coefficients $a(t)$ and $\bar{a}(t)$

$$i \frac{d}{dt} \begin{bmatrix} a(t) \\ \bar{a}(t) \end{bmatrix} = \begin{bmatrix} H_{11} & H_{12} \\ H_{21} & H_{22} \end{bmatrix} \begin{bmatrix} a(t) \\ \bar{a}(t) \end{bmatrix}. \tag{2.15}$$

The matrix H_{ij} is given by matrix elements of H_{weak} between eigenstates of H_s . Its decomposition into hermitian and antihermitian parts reads $H_{ij} = M_{ij} - \frac{i}{2} \Gamma_{ij}$, with $M = M^\dagger$ and $\Gamma = \Gamma^\dagger$. One usually imposes

$$\text{CPT } |B^0\rangle = |\bar{B}^0\rangle \quad \text{and} \quad \text{CP } |B^0\rangle = |\bar{B}^0\rangle \tag{2.16}$$

to fix convention-dependent phases in the relative normalization of B^0 and \bar{B}^0 . Under such conventions, CPT conservation implies $H_{11} = H_{22} \equiv D$, while $H_{12} \neq H_{21}$ implies CP violation. The eigenvalues and eigenvectors of H_{ij} are easily found to be

$$\begin{aligned} \lambda_{H,L} &= m_{H,L} - \frac{i}{2} \Gamma_{H,L} = D \pm \sqrt{H_{12}} \sqrt{H_{21}}, \\ |B_{H,L}\rangle &= \frac{1}{\sqrt{2(1+|\kappa|^2)}} [(1+\kappa) |B^0\rangle \mp (1-\kappa) |\bar{B}^0\rangle] \end{aligned} \tag{2.17}$$

with $\kappa = (\sqrt{H_{12}} - \sqrt{H_{21}}) / (\sqrt{H_{12}} + \sqrt{H_{21}})$. The state $|\Psi(t)\rangle$ (2.13) can now be written as

$$|\Psi(t)\rangle = c_L e^{-im_H t - \Gamma_H t/2} |B_H\rangle + c_S e^{-im_L t - \Gamma_L t/2} |B_L\rangle + \sum_n b_n(t) |n\rangle \tag{2.18}$$

with the coefficients c_L and c_S adjusted to match the initial condition $|\Psi(t_0)\rangle = |B^0\rangle$.

The eigenstate $|B_H\rangle$ becomes CP-odd in the limit of no CP violation. The mass and width differences of the two eigenstates are denoted by $\Delta m_d = m_H - m_L$ and $\Delta\Gamma_d = \Gamma_H - \Gamma_L$. Their measured values [7] and the corresponding SM predictions [8] (in units ps^{-1}) are given below together with the analogous quantities (Δm_s and $\Delta\Gamma_s$) for the B_s - \bar{B}_s system

$$\begin{aligned} \Delta m_d &= \begin{cases} (0.5064 \pm 0.0019)^{\text{exp}}, \\ (0.528 \pm 0.078)^{\text{SM}}, \end{cases} & \Delta\Gamma_d &= \begin{cases} [(-1.3 \pm 6.6) \times 10^{-3}]^{\text{exp}}, \\ [(2.61 \pm 0.59) \times 10^{-3}]^{\text{SM}}, \end{cases} \\ \Delta m_s &= \begin{cases} (17.757 \pm 0.021)^{\text{exp}}, \\ (18.3 \pm 2.7)^{\text{SM}}, \end{cases} & \Delta\Gamma_s &= \begin{cases} [(8.6 \pm 0.6) \times 10^{-2}]^{\text{exp}}, \\ [(8.8 \pm 2.0) \times 10^{-2}]^{\text{SM}}. \end{cases} \end{aligned} \quad (2.19)$$

In the quoted SM predictions for $\Delta m_{d,s}$, the necessary CKM parameters were determined from the fit as in Fig. 1, but excluding the input from the very mass differences $\Delta m_{d,s}$. This is one of the reasons why the predictions are by far less accurate than the measurements. Another reason are the uncertainties stemming from lattice QCD estimates of the relevant matrix elements of H_{weak} between the neutral B -meson states. Conversely, one of the main sources of uncertainty in the constraint from $\Delta m_d/\Delta m_s$ in Fig. 1 comes from the necessary lattice inputs.

Comparing $\Delta\Gamma_{d,s}$ to the actually measured total widths [7] $\Gamma_d^H \simeq \Gamma_d^L = 0.658(2)$, $\Gamma_s^L = 0.707(3)$, $\Gamma_s^H = 0.622(4)$, one concludes that the width difference in the B_s - \bar{B}_s system is sizeable, contrary to the B_d - \bar{B}_d case. This fact allows to study interesting time-dependent effects in B_s decays that might be potentially sensitive to BSM effects (see, *e.g.*, Ref. [9]).

2.4. The semileptonic CP asymmetry

CP violation in the B_q - \bar{B}_q mixing alone is parameterized by a single parameter that can be chosen to be $\text{Im}(\Gamma_{12}^q/M_{12}^q)$. It gives rise to CP asymmetries in decays to flavour-specific eigenstates f

$$A_{\text{fs}}^q \equiv A_{\text{sl}}^q = \frac{\Gamma(\bar{B}_q(t) \rightarrow f) - \Gamma(B_q(t) \rightarrow \bar{f})}{\Gamma(\bar{B}_q(t) \rightarrow f) + \Gamma(B_q(t) \rightarrow \bar{f})} = \text{Im}\left(\frac{\Gamma_{12}^q}{M_{12}^q}\right). \quad (2.20)$$

Here, $B_q(t)$ ($\bar{B}_q(t)$) stands for the state that was produced as B_q (\bar{B}_q) at $t = 0$, and then evolved according to Eq. (2.18). The final state f is called flavour-specific if it can arise (at the leading order in the electroweak interactions) only in decays of the b quark. The state \bar{f} is the CP conjugate of f . For final states f containing $D_s^+(c\bar{s})$ or $D^+(c\bar{d})$, examples of flavour-specific decays are $\bar{B}_s \rightarrow D_s^+ \pi^-$ or $\bar{B}_d \rightarrow D^+ \mu^- \bar{\nu}_\mu$, respectively, as they can

only occur via the $b \rightarrow cW^{*-}$ transition. On the other hand, $\bar{B}_d \rightarrow D^+\pi^-$ ($\bar{B}_s \rightarrow D_s^+K^-$) is not flavour-specific because the same final state could be obtained without mixing from B_d (B_s) via the decay channel $\bar{b} \rightarrow \bar{u}W^{+*}$ followed by $W^{+*} \rightarrow c\bar{d}$ ($W^{+*} \rightarrow c\bar{s}$).

The asymmetries in Eq. (2.20) are called the semileptonic CP asymmetries, as the most obvious flavour-specific states arise in the semileptonic decays. These asymmetries are related to the inclusive dimuon asymmetry measured by D0 in $p\bar{p}$ collisions [6]

$$A_{\text{sl}}^b = \frac{N_b^{++} - N_b^{--}}{N_b^{++} + N_b^{--}} = 0.506(43) A_{\text{sl}}^d + 0.494(43) A_{\text{sl}}^s, \quad (2.21)$$

where N_b^{++} (N_b^{--}) stand for numbers of same-charge $\mu^+\mu^+$ ($\mu^-\mu^-$) from events involving $B_q^0 \rightarrow \mu X$ decays. Actually, D0 performs an inclusive measurement without verifying whether any of the muons comes from the neutral B -meson decays. However, the $B-\bar{B}$ mixing seems to be the most likely explanation, and only such a hypothesis is going to be considered here. Since the initial state is CP-symmetric, a non-zero value of A_{sl}^b implies CP violation, provided one properly subtracts all the effects of the fact that the detector is not CP-symmetric. The latter effects are indeed carefully subtracted using measurements of single-muon asymmetries in the same experimental setup.

The numbers multiplying A_{sl}^d and A_{sl}^s in Eq. (2.21) come from the relative B_d and B_s production rates at D0. The measurement of A_{sl}^b gives us a constraint in the $(A_{\text{sl}}^d, A_{\text{sl}}^s)$ plane. A summary [7] of current constraints in this plane (from all the available measurements) is shown in Fig. 3. The D0 inclusive measurements with muons give rise to the ellipse marked ‘‘D0 muons’’. If taken on their own, they show a 3.6σ deviation from the SM prediction [8]

$$\begin{aligned} A_{\text{sl}}^d &= -4.7(6) \times 10^{-4} \sim \text{Im} \left(\frac{V_{ud}^* V_{ub}}{V_{td}^* V_{tb}} \right), \\ A_{\text{sl}}^s &= 2.22(27) \times 10^{-5} \sim \text{Im} \left(\frac{V_{us}^* V_{ub}}{V_{ts}^* V_{tb}} \right) \end{aligned} \quad (2.22)$$

that lies very close to $(0, 0)$. However, exclusive measurements of D0 and LHCb point towards different regions in the considered plane, and eventually the world average central value is only around 1σ away from the SM point. Nevertheless, the situation is not yet conclusive given that the constraints from various measurements are not really consistent with each other. The LHCb measurement is $\sim 2.2\sigma$ away from the average of the D0 measurements (the dashed ellipse). If at least the exclusive measurements alone

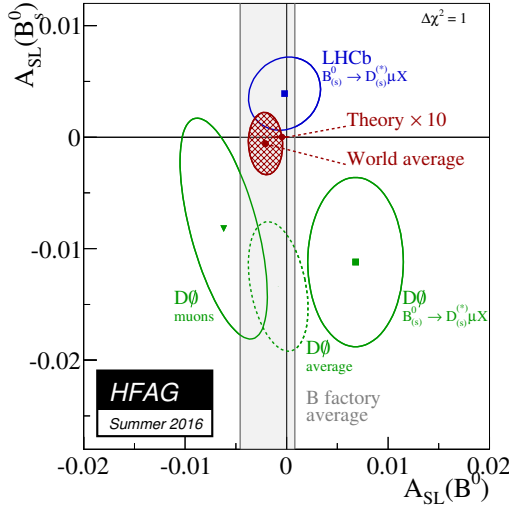


Fig. 3. Current status of the semileptonic CP asymmetry measurements [7].

agreed with each other, we could perhaps seriously consider that the inclusive dimuon asymmetry has another (BSM) source than the $B-\bar{B}$ mixing. So long as it does not happen, either underestimations of systematic uncertainties or statistical fluctuations seem to be the most likely explanations for the observed tensions in the data.

3. $B_{s,d} \rightarrow \ell^+ \ell^-$ in the SM

Let us now turn to the $B_q \rightarrow \ell^+ \ell^-$ branching ratios ($q = s, d$), for which a significant progress in the accuracy of SM predictions has recently been achieved [10, 11]. The calculations are conveniently performed in the framework of an effective theory, where the relevant weak interactions come in the form of a single four-fermion vertex

$$\mathcal{H}_{\text{int}} = -N C_A(\mu) (\bar{b} \gamma_\alpha \gamma_5 q) (\bar{\ell} \gamma^\alpha \gamma_5 \ell) . \tag{3.1}$$

The Wilson coefficient C_A is $\overline{\text{MS}}$ -renormalized at the scale μ . It contains all the relevant information on electroweak loop diagrams (dressed with perturbative gluons) that mediate the considered transition. Non-perturbative QCD effects arise only when H_{int} is inserted between the B -meson state at rest and the final leptonic state. In the normalization constant $N = V_{tb}^* V_{tq} (G_F M_W / \pi)^2$, the Fermi constant G_F is multiplied by the on-shell mass M_W .

The value of C_A is found using the so-called matching calculations which rely on the requirement that the perturbative amplitudes generated by H_{int} reproduce the full SM ones at the electroweak renormalization scale $\mu_0 \sim m_t$.

Such calculations for C_A at the three-loop level in QCD [10] and at the two-loop level in the electroweak interactions [11] were performed using off-shell amplitudes and expansions in external momenta. Next, the renormalization group running from μ_0 to $\mu \sim m_b$ was applied to resum the leading QED logarithms.

Once $C_A(\mu)$ is determined, the average time-integrated branching ratio $\overline{B}_{q\ell}$ of the $B_q \rightarrow \ell^+\ell^-$ decay is expressed in terms of the lepton mass m_ℓ , the B_q -meson mass M_{B_q} and its decay constant f_{B_q} . The latter is defined by the QCD matrix element $\langle 0|\bar{b}\gamma^\alpha\gamma_5q|B_q(p)\rangle = ip^\alpha f_{B_q}$. A simple calculation gives

$$\overline{B}_{q\ell} = \frac{|N|^2 M_{B_q}^3 f_{B_q}^2}{8\pi \Gamma_H^q} \beta_{q\ell} r_{q\ell}^2 |C_A(\mu)|^2 + \mathcal{O}(\alpha_{\text{em}}), \tag{3.2}$$

where Γ_H^q comes from Eq. (2.18), $r_{q\ell} = 2m_\ell/M_{B_q}$, and $\beta_{q\ell} = \sqrt{1 - r_{q\ell}^2}$.

The $\mathcal{O}(\alpha_{\text{em}})$ term in Eq. (3.2) is going to be neglected despite including complete corrections of this order to $C_A(\mu)$. One justifies such an approach by observing that some of the $\mathcal{O}(\alpha_{\text{em}})$ corrections to $C_A(\mu)$ get enhanced by $M_Z^2/(M_Z^2 - M_W^2)$, powers of m_t^2/M_W^2 or logarithms $\ln^2 M_W^2/\mu^2$. None of these enhancements is possible for the $\mathcal{O}(\alpha_{\text{em}})$ term in Eq. (3.2) once $\mu \sim m_b$. This term is μ -dependent and contains contributions from vertices (operators) like $(\bar{b}\gamma_\alpha\gamma_5q)(\bar{\ell}\gamma^\alpha\ell)$ or $(\bar{b}\gamma_\alpha P_L c)(\bar{c}\gamma^\alpha P_L s)$, with photons connecting the quark and lepton lines. It depends on non-perturbative QCD in a way that is not described by f_{B_q} alone, and it must compensate the μ -dependence of $C_A(\mu)$. Since this term is neglected, renormalization-scale dependence serves as one of the uncertainty estimates. When μ is varied from $m_b/2$ to $2m_b$, the results for $|C_A(\mu)|^2$ vary by about 0.3%, which corresponds to a typical size of $\mathcal{O}(\alpha_{\text{em}})$ corrections that undergo no extra enhancement. On the other hand, the electroweak corrections to $|C_A(\mu)|^2$ often reach a few percent level [11].

With the numerical inputs collected in Table 1 of Ref. [12], one obtains for the $\overline{B}_{s\mu}$ branching ratio

$$\overline{B}_{s\mu} \times 10^9 = (3.65 \pm 0.06) R_{t\alpha} R_s = 3.65 \pm 0.23, \tag{3.3}$$

where

$$R_{t\alpha} = [M_t/(173.1 \text{ GeV})]^{3.06} [\alpha_s(M_Z)/0.1184]^{-0.18} \tag{3.4}$$

and

$$R_s = \left(\frac{f_{B_s} [\text{MeV}]}{227.7} \right)^2 \left(\frac{|V_{cb}|}{0.0424} \right)^2 \left(\frac{|V_{tb}^* V_{ts}/V_{cb}|}{0.980} \right)^2 \frac{\tau_H^s [\text{ps}]}{1.615}, \tag{3.5}$$

with $\tau_H^s = 1/\Gamma_H^s$. Uncertainties due to parameters that do not occur in the quantities R_α , R_t and R_s have been absorbed into the residual error in the

middle term of Eq. (3.3). This residual error is actually dominated by a non-parametric uncertainty, which is estimated to constitute around 1.5% of the branching ratio. A reduction of the very non-parametric uncertainty from around 8% to the current level was the main purpose for the $\mathcal{O}(\alpha_s^2, \alpha_{em})$ matching calculations in Refs. [10, 11].

All the other $\bar{\mathcal{B}}_{q\ell}$ branching ratios are calculated along the same lines. One finds

$$\begin{aligned}
 \bar{\mathcal{B}}_{se} \times 10^{14} &= (8.54 \pm 0.13) R_{t\alpha} R_s = 8.54 \pm 0.55, \\
 \bar{\mathcal{B}}_{s\tau} \times 10^7 &= (7.73 \pm 0.12) R_{t\alpha} R_s = 7.73 \pm 0.49, \\
 \bar{\mathcal{B}}_{de} \times 10^{15} &= (2.48 \pm 0.04) R_{t\alpha} R_d = 2.48 \pm 0.21, \\
 \bar{\mathcal{B}}_{d\mu} \times 10^{10} &= (1.06 \pm 0.02) R_{t\alpha} R_d = 1.06 \pm 0.09, \\
 \bar{\mathcal{B}}_{d\tau} \times 10^8 &= (2.22 \pm 0.04) R_{t\alpha} R_d = 2.22 \pm 0.19
 \end{aligned}
 \tag{3.6}$$

with

$$R_d = \left(\frac{f_{B_d} [\text{MeV}]}{190.5} \right)^2 \left(\frac{|V_{tb}^* V_{td}|}{0.0088} \right)^2 \frac{\tau_d^{\text{av}} [\text{ps}]}{1.519}.
 \tag{3.7}$$

A summary of the error budgets for $\bar{\mathcal{B}}_{s\ell}$ and $\bar{\mathcal{B}}_{d\ell}$ is presented in Table II. It is clear that the main parametric uncertainties come from f_{B_q} and the CKM angles.

TABLE II

Relative uncertainties from various sources in $\bar{\mathcal{B}}_{s\ell}$ and $\bar{\mathcal{B}}_{d\ell}$. In the last column, they are added in quadrature.

	f_{B_q}	CKM	τ_H^q	M_t	α_s	Other param.	Non-param.	Σ
$\bar{\mathcal{B}}_{s\ell}$	4.0%	4.3%	1.3%	1.6%	0.1%	< 0.1%	1.5%	6.4%
$\bar{\mathcal{B}}_{d\ell}$	4.5%	6.9%	0.5%	1.6%	0.1%	< 0.1%	1.5%	8.5%

For $\ell = \mu$, the SM predictions can be compared with the latest LHCb measurement [13]

$$\bar{\mathcal{B}}_{s\mu} = (3.0 \pm 0.6_{-0.2}^{+0.3}) \times 10^{-9}, \quad \bar{\mathcal{B}}_{d\mu} = (1.5_{-1.0-0.1}^{+1.2+0.2}) \times 10^{-10},
 \tag{3.8}$$

where the first error is statistical, and the second — systematic. It follows that both measurements agree with the SM prediction within 1σ . In the $\bar{\mathcal{B}}_{s\mu}$ case, a reduction of experimental uncertainties to a few percent level is expected in the forthcoming decade.

4. Anomalies in $B \rightarrow K^{(*)}\ell^+\ell^-$ and $B \rightarrow D^{(*)}\tau\nu$

While just a single effective vertex (3.1) was sufficient for each of the $B_q \rightarrow \ell^+\ell^-$ decays in the SM, many more such vertices matter for $B \rightarrow K^{(*)}\ell^+\ell^-$ with $\ell = e, \mu$. The relevant loop-generated ones in the SM take the form of

$$Q_7 \sim (\bar{s}_L \sigma_{\alpha\beta} b_R) F^{\alpha\beta}, \quad Q_9^{(\ell)} \sim (\bar{s}_L \gamma^\alpha b_L)(\bar{\ell} \gamma_\alpha \ell), \quad Q_{10}^{(\ell)} \sim (\bar{s}_L \gamma^\alpha b_L)(\bar{\ell} \gamma_\alpha \gamma_5 \ell). \tag{4.1}$$

Interaction (3.1) for B_s was actually a part² of $Q_{10}^{(\ell)}$. Thus, possible BSM contributions to the Wilson coefficient $Q_{10}^{(\mu)}$ are already constrained by the agreement of the SM prediction for $\bar{B}_{s\mu}$ (3.3) with the experimental result (3.8). The same is true for the Wilson coefficient of Q_7 that receives tight constraints from radiative decays — see Section 5. On the other hand, global analyses of $B \rightarrow K^{(*)}\ell^+\ell^-$ data show deviations from the SM that can be explained by introducing a BSM contribution proportional solely to $Q_9^{(\mu)}$.

Before discussing the considered observables, let us have a look at final results of two of such global analyses [14, 15]. They are presented in Fig. 4 as plots of allowed regions in the $(C_9^{\text{NP}}, C_{10}^{\text{NP}})$ plane, with C_k^{NP} denoting a hypothetical BSM contribution to the Wilson coefficient of $Q_k^{(\mu)}$. Such BSM contributions are supposed to be initially determined at $\mu_0 \sim m_t$, and then evolved down to a scale of the order of m_b . However, their renormalization group running is very mild (it is due to QED only), and can be safely neglected when compared to other uncertainties in Fig. 4.

The SM point (0, 0) is visibly outside the allowed regions in both plots of Fig. 4. In the left plot, the dark- and light-grey/blue regions correspond to the 1σ and 2σ ranges, respectively, while the “pull” between the best fit point and the SM one amounts to 3.8σ . In the right plot, the three grey/red contours correspond to $1, 2, 3\sigma$, while the pull amounts to 4.3σ . In more recent articles (see, *e.g.*, Ref. [16]), deviations from the SM at the 5σ level are found³. However, the statistical significance of the fits needs to be taken with a grain of salt. Let us explain the issue in more detail.

The fits include observables from all the available processes involving the $b \rightarrow s\gamma$ and $b \rightarrow s\ell^+\ell^-$ transitions. Thus, constraints from $B_s \rightarrow \mu^+\mu^-$ and $\bar{B} \rightarrow X_s\gamma$ (that agree with the SM) are taken into account. The largest deviations occur in angular observables of $B \rightarrow K^*\ell^+\ell^-$ whose theoretic-

² The vector part of the quark current was dropped for simplicity, as it does not contribute to $B_q \rightarrow \ell^+\ell^-$.

³ The pulls do depend, though not very sensitively, on whether $(C_9^{\text{NP}}, C_{10}^{\text{NP}})$ are the only allowed BSM contributions (as in Fig. 4), or we admit other operators to acquire BSM Wilson coefficients. This includes operators whose Wilson coefficients vanish or are negligible in the SM.

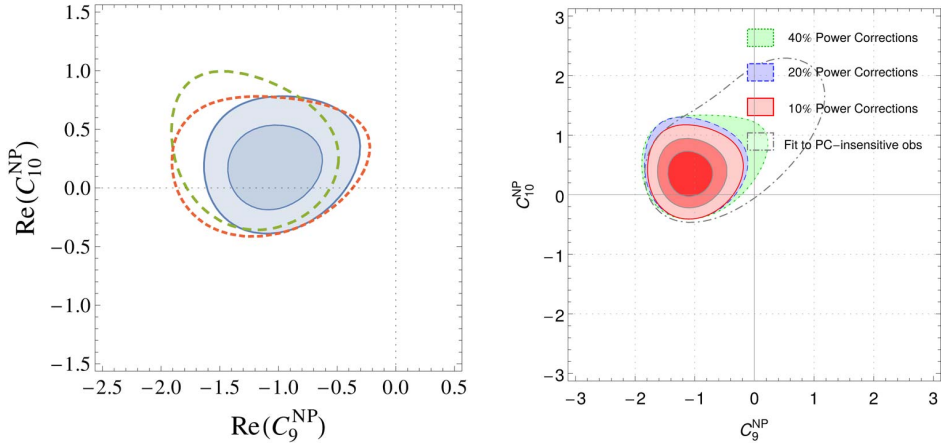


Fig. 4. (Colour on-line) Constraints in the $(C_9^{\text{NP}}, C_{10}^{\text{NP}})$ plane from global fits to $b \rightarrow s\ell^+\ell^-$ and $b \rightarrow s\gamma$ observables. The plots are from Fig. 4b of Ref. [14] and Fig. 15b of Ref. [15] (right).

cal analysis is strongly dependent on our understanding of non-perturbative QCD effects in exclusive “heavy-to-light” decays. If only operators (4.1) were present, one could form observables in which the non-perturbative form factors cancel out up to $\mathcal{O}(\Lambda_{\text{QCD}}/m_b)$ corrections, while the very corrections can be estimated using either the light-cone sum rules or lattice QCD simulations. However, one also needs to take into account four quark operators of the form $(\bar{s}_L\gamma^\alpha c_L)(\bar{c}_L\gamma_\alpha b_L)$ whose perturbative contributions via charm-quark loops [17, 18] affect C_9 by more than the BSM effects implied by the fits. It is difficult to disentangle such perturbative effects from non-perturbative ones that come as the so-called “continuum contributions” in the light-cone sum rule analyses [19]. Thus, one should be very careful about identifying BSM physics in such contributions to C_9 that resemble the perturbative charm loop effects.

An important property of the charm loop effects is that the lepton pair is produced by a virtual photon, which implies lepton flavour universality (LFU). On the other hand, an evidence for LFU violation at the level of $2\text{--}3\sigma$ does show up in the LHCb measurements of the ratios

$$R_{K^{(*)}} = \frac{\mathcal{B}(B \rightarrow K^{(*)}\mu^+\mu^-)}{\mathcal{B}(B \rightarrow K^{(*)}e^+e^-)} = \begin{cases} 0.745_{-0.074}^{+0.090} \pm 0.036, & \text{for } K \text{ [20]}, \\ 0.69_{-0.07}^{+0.11} \pm 0.05, & \text{for } K^* \text{ [21]} \end{cases} \quad (4.2)$$

in the dimuon invariant mass ranges of $[1.0, 6.0]$ and $[1.1, 6.0]$ GeV^2 , respectively. In these ranges, the leptons can be treated as practically massless, which implies that R_K and R_{K^*} are predicted to be very close to unity in the SM (within $\pm 1\%$) due to flavour universality of the lepton-(gauge

boson) couplings. Thus, if there is no BSM contribution, the only alternative remains on the experimental side, which might be either a statistical fluctuation or systematic effects.

What many people find intriguing is that explaining R_K and R_{K^*} via BSM contributions to $C_9^{(\mu)}$ transitions (while keeping $C_9^{(e)}$ at the SM level) is perfectly consistent with what we need to match the angular observables in $B \rightarrow K^* \mu^+ \mu^-$ with experiment, without introducing any enlarged non-perturbative uncertainty due to the charm loops over what has been estimated in Ref. [19]. Nevertheless, in my opinion, we should still treat the $b \rightarrow s \ell^+ \ell^-$ anomalies as $\sim 3\sigma$ rather than $\sim 5\sigma$ ones.

There is a whole spectrum of models that have been considered to explain BSM contributions to $C_9^{(\mu)}$. The simplest ones assume existence of a heavy U(1) gauge boson with flavour-violating couplings. It could be as heavy as 10 TeV and give no currently observable effects in anything but $C_9^{(\mu)}$. Another possibility are heavy scalar leptoquarks that could contribute to Q_9 and Q_{10} thanks to the Fierz identities like $(\bar{s}_L \mu_R)(\mu_R b_L) \sim (\bar{s}_L \gamma^\alpha b_L)(\mu_R \gamma_\alpha \mu_R)$.

The leptoquark option might be considered more attractive (see, *e.g.*, Ref. [22]) in view of another ‘‘anomaly’’ that suggests LFU violation. A 3.9σ deviation from the SM is observed in the quantities

$$R_{D^{(*)}} = \frac{\mathcal{B}(B \rightarrow D^{(*)} \tau \nu)}{\mathcal{B}(B \rightarrow D^{(*)} \mu \nu)}, \tag{4.3}$$

as illustrated in Fig. 5. In this case, the SM prediction (the small grey ellipse) differs from unity due to non-negligible mass of the τ lepton. The

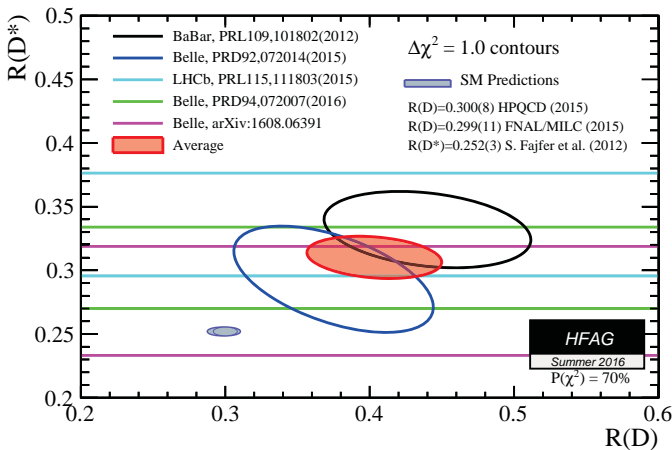


Fig. 5. Current experimental constraints in the R_D - R_{D^*} plane and their comparison to the SM prediction (Fig. 66 of Ref. [7]).

non-perturbative form factors that are necessary to evaluate the SM predictions for $R_{D^{(*)}}$ are extracted from the measured spectra of $B \rightarrow D^{(*)}\mu\nu$, except for a single one in the R_{D^*} case that, however, turns out to give a small contribution. The calculation is well-controlled for R_D (for which the discrepancy with the measurements is less severe), while a more uncertain theoretical input is necessary in the R_{D^*} case. Nevertheless, the experimental uncertainties are by far the dominant.

To conclude this section, I believe that the observed anomalies provide interesting hints for BSM physics, but it is still too early to claim a breakdown of the SM.

5. $\bar{B} \rightarrow X_{s,d}\gamma$ in the SM

The inclusive decays $\bar{B} \rightarrow X_s\gamma$ and $\bar{B} \rightarrow X_d\gamma$ provide important bounds on many popular BSM models. Evaluation of such bounds depends quite sensitively on the branching ratio predictions within the SM. An update of these predictions was presented in Ref. [23] which we shall follow below.

Measurements of the CP- and isospin-averaged $\bar{B} \rightarrow X_s\gamma$ branching ratio lead to the combined result (see Ref. [24] and references therein)

$$\mathcal{B}_{s\gamma}^{\text{exp}} = (3.27 \pm 0.14) \times 10^{-4}, \quad (5.1)$$

for the photon energy $E_\gamma > E_0 = 1.6$ GeV in the decaying meson rest frame. The combination involves an extrapolation from measurements performed at $E_0 = 1.9$ GeV. Applying the same extrapolation method [25] to the available $\bar{B} \rightarrow X_d\gamma$ measurement [26], one finds

$$\mathcal{B}_{d\gamma}^{\text{exp}} = (1.41 \pm 0.57) \times 10^{-5} \quad (5.2)$$

at $E_0 = 1.6$ GeV [27]. More precise determinations of $\mathcal{B}_{q\gamma}^{\text{exp}}$ for $q = s, d$ are expected from Belle II [28].

Theoretical calculations of $\mathcal{B}_{q\gamma}$ have a chance to match the experimental precision only in a certain range of E_0 where the non-perturbative contribution $\delta\Gamma_{\text{nonp}}$ in the relation

$$\Gamma(\bar{B} \rightarrow X_q\gamma) = \Gamma(b \rightarrow X_q^p\gamma) + \delta\Gamma_{\text{nonp}} \quad (5.3)$$

remains under control. Here, $\Gamma(b \rightarrow X_q^p\gamma)$ denotes the perturbatively calculable rate of the radiative b -quark decay involving only charmless partons in the final state. The analysis of Ref. [29] implies that unknown contributions to $\delta\Gamma_{\text{nonp}}$ are potentially larger than the so-far determined ones, and induce around $\pm 5\%$ uncertainty in $\mathcal{B}_{s\gamma}$ at $E_0 = 1.6$ GeV. Non-perturbative uncertainties in $\mathcal{B}_{d\gamma}$ receive additional sizeable contributions [30] due to collinear photon emission in the $b \rightarrow du\bar{u}\gamma$ process.

Apart from possible future progress in analyzing non-perturbative effects, one needs to determine $\Gamma(b \rightarrow X_q^p \gamma)$ to a few percent accuracy. It requires evaluating the Next-to-Next-to-Leading Order (NNLO) QCD corrections that involve Feynman diagrams up to four loops. The first SM estimate of the $\bar{B} \rightarrow X_s \gamma$ branching ratio at this level was presented in Ref. [31]. A part of the $\mathcal{O}(\alpha_s^2)$ contribution was obtained via interpolation [32] in the charm quark mass between the large- m_c asymptotic expression [33] and the $m_c = 0$ boundary condition that was estimated using the Brodsky–Lepage–Mackenzie (BLM) approximation [34]. The phenomenological update of Ref. [23] includes all the contributions and estimates worked out after the completion of Ref. [31]. The interpolation in m_c is still being applied. However, the $m_c = 0$ boundary condition is no longer a BLM-based estimate but rather comes from an explicit calculation [35].

Flavour-changing weak interactions that matter for $\Gamma(b \rightarrow X_q^p \gamma)$ with $q = s, d$ are given by the following effective Lagrangian:

$$\mathcal{L}_{\text{eff}} \sim V_{tq}^* V_{tb} \left[\sum_{i=1}^8 C_i Q_i + \kappa_q \sum_{i=1}^2 C_i (Q_i - Q_i^u) \right]. \quad (5.4)$$

Explicit expressions for the current–current ($Q_{1,2}$), four-quark penguin ($Q_{3,\dots,6}$), photonic dipole (Q_7), and gluonic dipole (Q_8) operators can be found, *e.g.*, in Eq. (2.5) of Ref. [32]. The CKM element ratio $\kappa_q = (V_{uq}^* V_{ub}) / (V_{tq}^* V_{tb})$ is small for $q = s$, and it affects $\mathcal{B}_{s\gamma}$ by less than 0.3%. Barring this effect and the higher-order electroweak ones, $\Gamma(b \rightarrow X_s^p \gamma)$ in the SM is given by a quadratic polynomial in the Wilson coefficients C_i

$$\Gamma(b \rightarrow X_s^p \gamma) \sim \sum_{i,j=1}^8 C_i C_j G_{ij}. \quad (5.5)$$

In the updated analysis of Ref. [23], the NNLO Wilson coefficient calculation becomes complete after including the four-loop anomalous dimensions that describe $Q_{1,\dots,6} \rightarrow Q_8$ mixing under renormalization [36]. Effects of the charm and bottom quark masses in loops on the gluon lines in G_{77} [37], G_{78} [38] and $G_{(1,2)7}$ [39], as well as a complete calculation of G_{78} [40] are taken into account. Three- and four-body final-state contributions to G_{88} [41, 42] and $G_{(1,2)8}$ [42] are included in the BLM approximation. Four-body final-state contributions involving the penguin and $Q_{1,2}^u$ operators are taken into account at the Leading Order (LO) [43] and Next-to-Leading Order (NLO) [44]. Last but not least, the full NNLO calculation [35] of G_{17} and G_{27} at $m_c = 0$ serves as a boundary for interpolating their unknown parts in m_c .

Following the algorithm described in detail in Ref. [35], taking into account new non-perturbative effects [29, 45, 46], as well as the previously omitted parts of the NNLO BLM corrections [47], one arrives at the following SM prediction (with $E_0 = 1.6$ GeV):

$$\mathcal{B}_{s\gamma}^{\text{SM}} = (3.36 \pm 0.23) \times 10^{-4}. \quad (5.6)$$

Individual contributions to the total uncertainty are of non-perturbative ($\pm 5\%$), higher-order ($\pm 3\%$), interpolation ($\pm 3\%$) and parametric ($\pm 2\%$) origin. They are combined in quadrature.

To study the $\mathcal{B}_{d\gamma}$ case, one begins with inserting the proper CKM factors in Eq. (5.4). Using the CKM fits described in Section 2.2, one finds

$$\kappa_d = (0.007_{-0.011}^{+0.015}) + i(-0.404_{-0.014}^{+0.012}). \quad (5.7)$$

The small real part implies that the main κ_d -effect comes from $b \rightarrow du\bar{u}\gamma$ at the LO. In the first (rough) approximation, one evaluates the tree-level $b \rightarrow du\bar{u}\gamma$ diagrams retaining a common light-quark mass m_q inside the collinear logarithms [42], and varying m_b/m_q between $10 \sim m_B/m_K$ and $50 \sim m_B/m_\pi$ to estimate the uncertainty. The considered effect varies then from 2% to 11% of $\mathcal{B}_{d\gamma}$. A more involved analysis with the help of fragmentation functions gives a very similar range [30]. Including this contribution, one finds (for $E_0 = 1.6$ GeV)

$$\mathcal{B}_{d\gamma}^{\text{SM}} = (1.73_{-0.22}^{+0.12}) \times 10^{-5}, \quad (5.8)$$

where the central value corresponds to $m_b/m_q = 50$.

Comparing Eqs. (5.1) and (5.2) with (5.6) and (5.8), respectively, one observes a very good agreement between the measurements and the SM predictions. The achieved precision in $\mathcal{B}_{s\gamma}$ tightly constraints the coefficient C_7 , leaving little freedom in this parameter in the fits discussed in Section 4.

6. Summary

With large amounts of B -physics data collected over the past years, subsequent surprises have arrived. First, we have not seen BSM effects where we had hoped for them to occur, namely in loop-generated observables where our calculations and measurements are sensitive to percent-level deviations from the SM. At present, we find 10–20% deviations in observables like $R_{D^{(*)}}$ that are generated by tree diagrams with no CKM suppression. As far as the loop-generated $C_9^{(\mu)}$ is concerned, the observed deviation is at the level of $\sim 25\%$ of the SM contribution, and appears to be LFU violating. Although several explicit BSM models that are consistent with

all the current surprises have been shown to exist, we should remain cautious with definite conclusions until either further indirect evidence is found or, hopefully, signals for real production of BSM particles are observed at the LHC.

REFERENCES

- [1] Y. Onishi, “Start of SuperKEKB”, plenary talk at the ICHEP 2016 Conference, Chicago, August 3–10, 2016.
- [2] B. Grzadkowski, M. Iskrzyński, M. Misiak, J. Rosiek, *J. High Energy Phys.* **1010**, 085 (2010) [arXiv:1008.4884 [hep-ph]].
- [3] J. Charles *et al.* [CKMfitter Group], *Eur. Phys. J. C* **41**, 1 (2005) [arXiv:hep-ph/0406184], updates at <http://ckmfitter.in2p3.fr>
- [4] M. Bona *et al.* [UTfit Collaboration], *J. High Energy Phys.* **0610**, 081 (2006) [arXiv:hep-ph/0606167], updates at <http://www.utfit.org/UTfit>
- [5] M. Blanke, A.J. Buras, *Eur. Phys. J. C* **76**, 197 (2016) [arXiv:1602.04020 [hep-ph]].
- [6] V.M. Abazov *et al.* [D0 Collaboration], *Phys. Rev. D* **89**, 012002 (2014) [arXiv:1310.0447 [hep-ex]].
- [7] Y. Amhis *et al.* [Heavy Flavor Averaging Group], arXiv:1612.07233 [hep-ex].
- [8] M. Artuso, G. Borissov, A. Lenz, *Rev. Mod. Phys.* **88**, 045002 (2016) [arXiv:1511.09466 [hep-ph]].
- [9] A.J. Buras, R. Fleischer, J. Girrbach, R. Knegjens, *J. High Energy Phys.* **1307**, 77 (2013) [arXiv:1303.3820 [hep-ph]].
- [10] T. Hermann, M. Misiak, M. Steinhauser, *J. High Energy Phys.* **1312**, 097 (2013) [arXiv:1311.1347 [hep-ph]].
- [11] C. Bobeth, M. Gorbahn, E. Stamou, *Phys. Rev. D* **89**, 034023 (2014) [arXiv:1311.1348 [hep-ph]].
- [12] C. Bobeth *et al.*, *Phys. Rev. Lett.* **112**, 101801 (2014) [arXiv:1311.0903 [hep-ph]].
- [13] R. Aaij *et al.* [LHCb Collaboration], *Phys. Rev. Lett.* **118**, 191801 (2017) arXiv:1703.05747 [hep-ex].
- [14] W. Altmannshofer, D.M. Straub, *Eur. Phys. J. C* **75**, 382 (2015) [arXiv:1411.3161 [hep-ph]].
- [15] S. Descotes-Genon, L. Hofer, J. Matias, J. Virto, *J. High Energy Phys.* **1606**, 092 (2016) [arXiv:1510.04239 [hep-ph]].
- [16] B. Capdevila *et al.*, arXiv:1704.05340 [hep-ph].
- [17] M. Misiak, *Nucl. Phys. B* **393**, 23 (1993) [Erratum *ibid.* **439**, 461 (1995)].
- [18] C. Bobeth, M. Misiak, J. Urban, *Nucl. Phys. B* **574**, 291 (2000) [arXiv:hep-ph/9910220].

- [19] A. Khodjamirian, T. Mannel, A.A. Pivovarov, Y.M. Wang, *J. High Energy Phys.* **1009**, 089 (2010) [arXiv:1006.4945 [hep-ph]].
- [20] R. Aaij *et al.* [LHCb Collaboration], *Phys. Rev. Lett.* **113**, 151601 (2014) [arXiv:1406.6482 [hep-ex]].
- [21] R. Aaij *et al.* [LHCb Collaboration], arXiv:1705.05802 [hep-ex].
- [22] D. Bečirević, S. Fajfer, N. Košnik, O. Sumensari, *Phys. Rev. D* **94**, 115021 (2016) [arXiv:1608.08501 [hep-ph]].
- [23] M. Misiak *et al.*, *Phys. Rev. Lett.* **114**, 221801 (2015) [arXiv:1503.01789 [hep-ph]].
- [24] M. Misiak, M. Steinhauser, *Eur. Phys. J. C* **77**, 201 (2017) [arXiv:1702.04571 [hep-ph]].
- [25] O.L. Büchmüller, H.U. Flächer, *Phys. Rev. D* **73**, 073008 (2006) [arXiv:hep-ph/0507253].
- [26] P. del Amo Sanchez *et al.* [BaBar Collaboration], *Phys. Rev. D* **82**, 051101 (2010) [arXiv:1005.4087 [hep-ex]].
- [27] A. Crivellin, L. Mercolli, *Phys. Rev. D* **84**, 114005 (2011) [arXiv:1106.5499 [hep-ph]].
- [28] T. Aushev *et al.*, arXiv:1002.5012 [hep-ex].
- [29] M. Benzke, S.J. Lee, M. Neubert, G. Paz, *J. High Energy Phys.* **1008**, 099 (2010) [arXiv:1003.5012 [hep-ph]].
- [30] H.M. Asatrian, C. Greub, *Phys. Rev. D* **88**, 074014 (2013) [arXiv:1305.6464 [hep-ph]].
- [31] M. Misiak *et al.*, *Phys. Rev. Lett.* **98**, 022002 (2007) [arXiv:hep-ph/0609232].
- [32] M. Misiak, M. Steinhauser, *Nucl. Phys. B* **764**, 62 (2007) [arXiv:hep-ph/0609241].
- [33] M. Misiak, M. Steinhauser, *Nucl. Phys. B* **840**, 271 (2010) [arXiv:1005.1173 [hep-ph]].
- [34] S.J. Brodsky, G.P. Lepage, P.B. Mackenzie, *Phys. Rev. D* **28**, 228 (1983).
- [35] M. Czakon *et al.*, *J. High Energy Phys.* **1504**, 168 (2015) [arXiv:1503.01791 [hep-ph]].
- [36] M. Czakon, U. Haisch, M. Misiak, *J. High Energy Phys.* **0703**, 008 (2007) [arXiv:hep-ph/0612329].
- [37] H.M. Asatrian, T. Ewerth, H. Gabrielyan, C. Greub, *Phys. Lett. B* **647**, 173 (2007) [arXiv:hep-ph/0611123].
- [38] T. Ewerth, *Phys. Lett. B* **669**, 167 (2008) [arXiv:0805.3911 [hep-ph]].
- [39] R. Boughezal, M. Czakon, T. Schutzmeier, *J. High Energy Phys.* **0709**, 072 (2007) [arXiv:0707.3090 [hep-ph]].
- [40] H.M. Asatrian *et al.*, *Phys. Rev. D* **82**, 074006 (2010) [arXiv:1005.5587 [hep-ph]].
- [41] A. Ferroglia, U. Haisch, *Phys. Rev. D* **82**, 094012 (2010) [arXiv:1009.2144 [hep-ph]].

- [42] M. Misiak, M. Poradziński, *Phys. Rev. D* **83**, 014024 (2011) [arXiv:1009.5685 [hep-ph]].
- [43] M. Kamiński, M. Misiak, M. Poradziński, *Phys. Rev. D* **86**, 094004 (2012) [arXiv:1209.0965 [hep-ph]].
- [44] T. Huber, M. Poradziński, J. Virto, *J. High Energy Phys.* **1501**, 115 (2015) [arXiv:1411.7677 [hep-ph]].
- [45] T. Ewerth, P. Gambino, S. Nandi, *Nucl. Phys. B* **830**, 278 (2010) [arXiv:0911.2175 [hep-ph]].
- [46] A. Alberti, P. Gambino, S. Nandi, *J. High Energy Phys.* **1401**, 147 (2014) [arXiv:1311.7381 [hep-ph]].
- [47] Z. Ligeti, M.E. Luke, A.V. Manohar, M.B. Wise, *Phys. Rev. D* **60**, 034019 (1999) [arXiv:hep-ph/9903305].